Supplementary Material

A cooling-driven self-adaptive and removable hydrogel coupled with combined chemo-photothermal sterilization for promoting infected wound healing

Jun Cao, ‡[a] Tao Zhang, ‡[b] Wei Zhu, [a] Hou-Bin Li [b] and Ai-Guo Shen *[a]

[a.]College of Chemistry and Chemical Engineering, Wuhan Textile University, Wuhan 430200, China.
E-mail address: agshen@wtu.edu.cn
[b.]Research Center of Graphic Communication, Printing and Packaging, Wuhan University, Wuhan 430079, China.
‡These authors contributed equally to this work.

Table S1. Parameter and gelation time of hydrogel samples.

Sample	PF127 (wt/vol)	rGO@PDA/Ag (mg mL^{-1})	Gelation time (s)
PF127	30%	0	120
rGO@PDA/Ag-PF127-1	30%	0.75	105
rGO@PDA/Ag-PF127-2	30%	1.50	95
rGO@PDA/Ag-PF127-3	30%	3.00	80

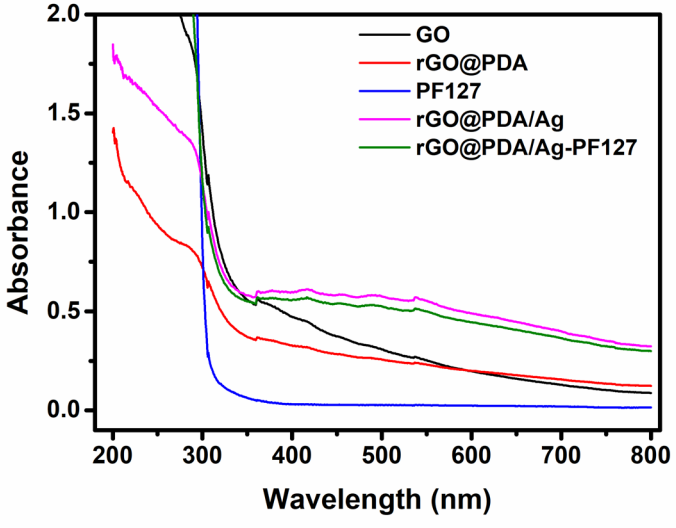

Fig. S1. UV-vis spectra of different samples.

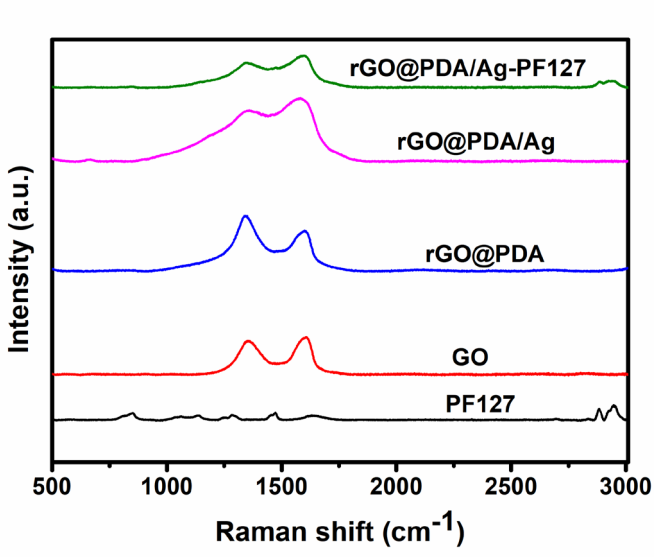

Fig. S2. Raman spectra of different samples (Laser wavelength: 532 nm).

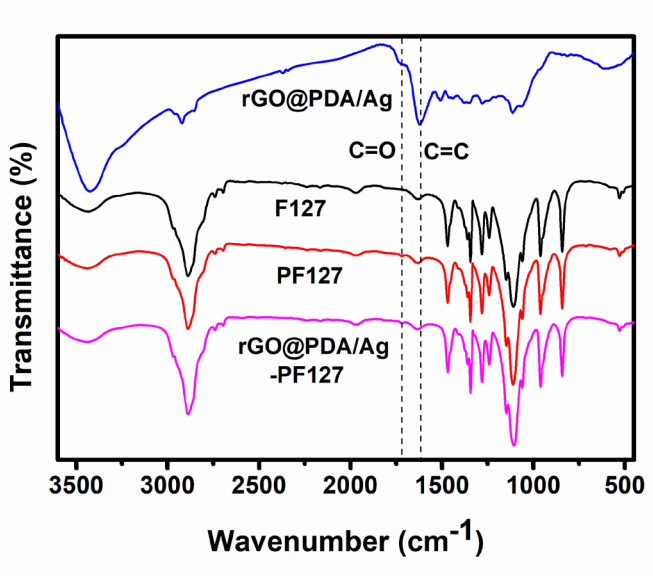

Fig. S3. FTIR spectra of different samples.

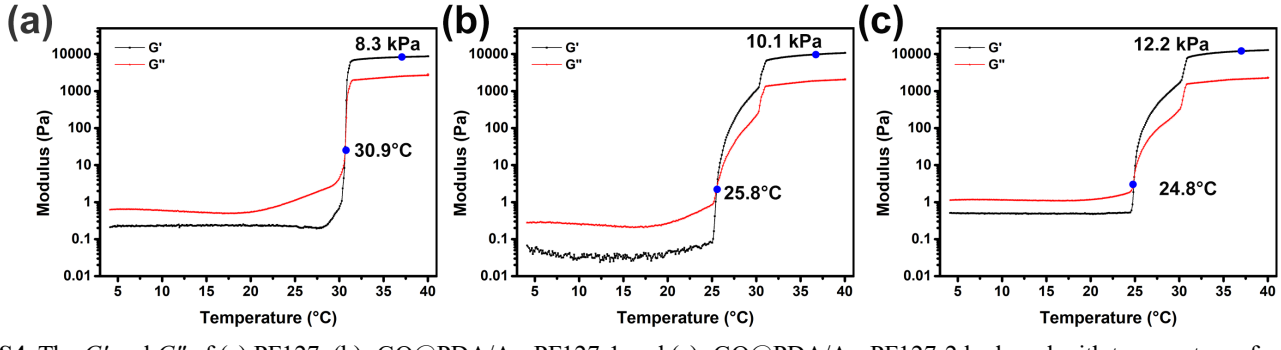

Fig. S4. The *G′* and *G″* of (a) PF127, (b) rGO@PDA/Ag-PF127-1 and (c) rGO@PDA/Ag-PF127-2 hydrogel with temperatures from 4 to 40°C

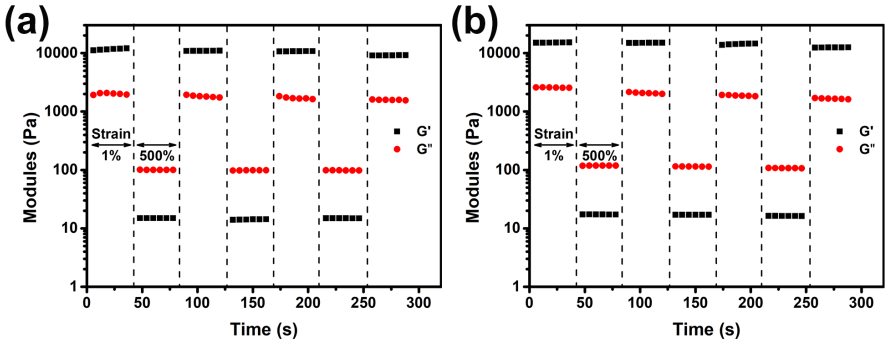

Fig. S5. Continuous step strain tests of (a) rGO@PDA/Ag-PF127-1 and (b) rGO@PDA/Ag-PF127-2 hydrogel under repeated deformation of 1% and 500% strain.

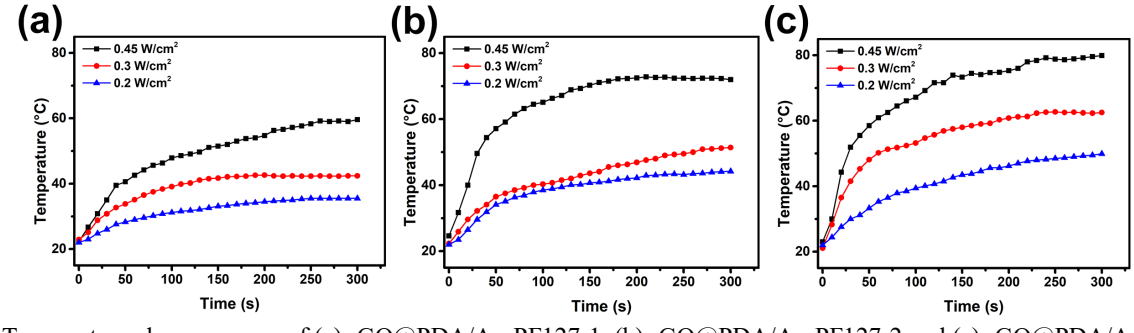

Fig. S6. Temperature change curves of (a) rGO@PDA/Ag-PF127-1, (b) rGO@PDA/Ag-PF127-2 and (c) rGO@PDA/Ag-PF127-3 hydrogels under the irradiation of laser with different laser power densities.

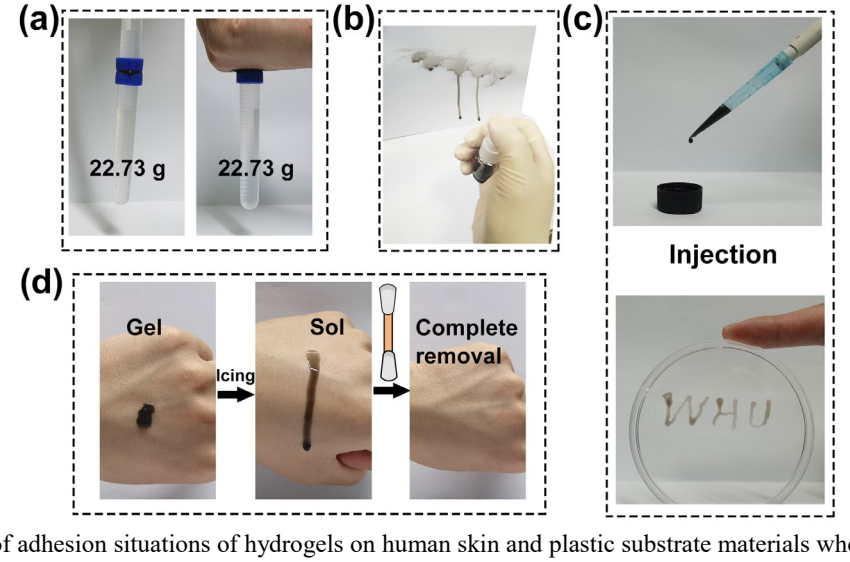

Fig. S7. (a) Photographs of adhesion situations of hydrogels on human skin and plastic substrate materials when bearing weight (22.73 g). (b) Images showing the sprayable properties of hydrogels. (c) Images illustrating sol-gel transformation ability of rGO@PDA/Ag-PF127-3 hydrogel. (d) Photographs of removability of hydrogels through gel-sol transition by ice bag.

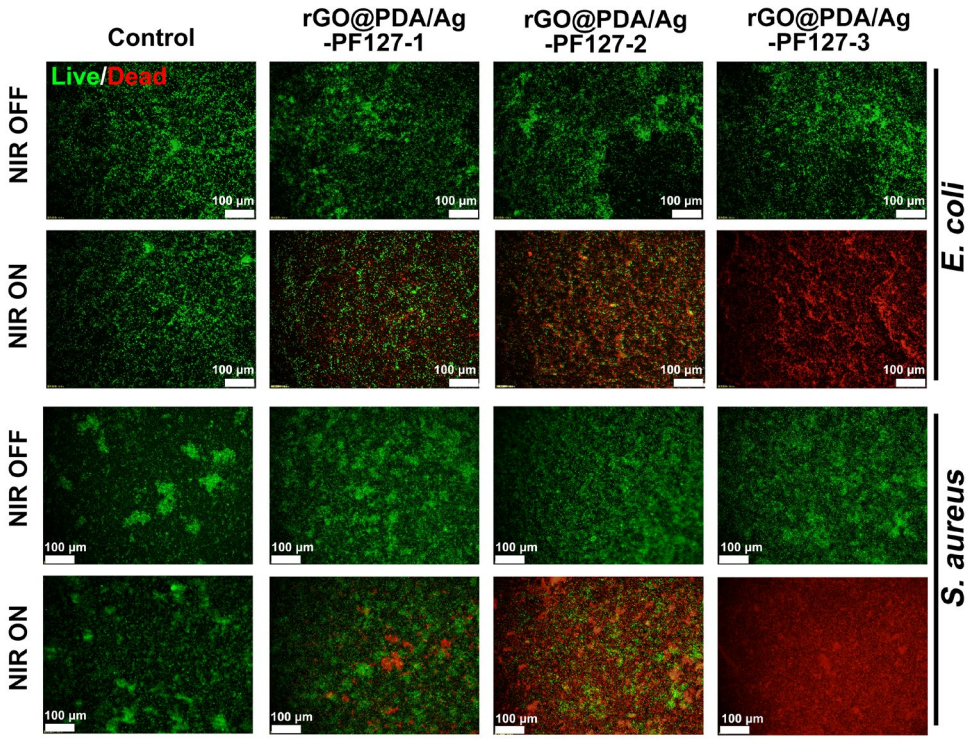

Fig. S8. Fluorescence images of *E. coli* and *S. aureus* stained with Calcein-AM/PI dyes after different treatments (Live bacteria stained green with Calcein-AM, and dead bacteria stained red with PI).

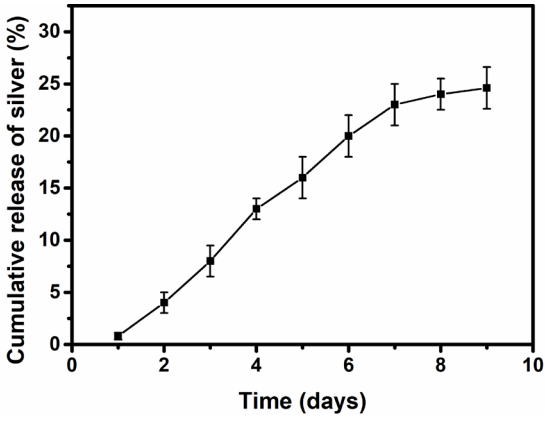

Fig. S9. The cumulative release curve of Ag^{+} in rGO@PDA/Ag-PF127-3 hydrogel at pH 7.4. Data are shown as mean ± SD, n = 3.

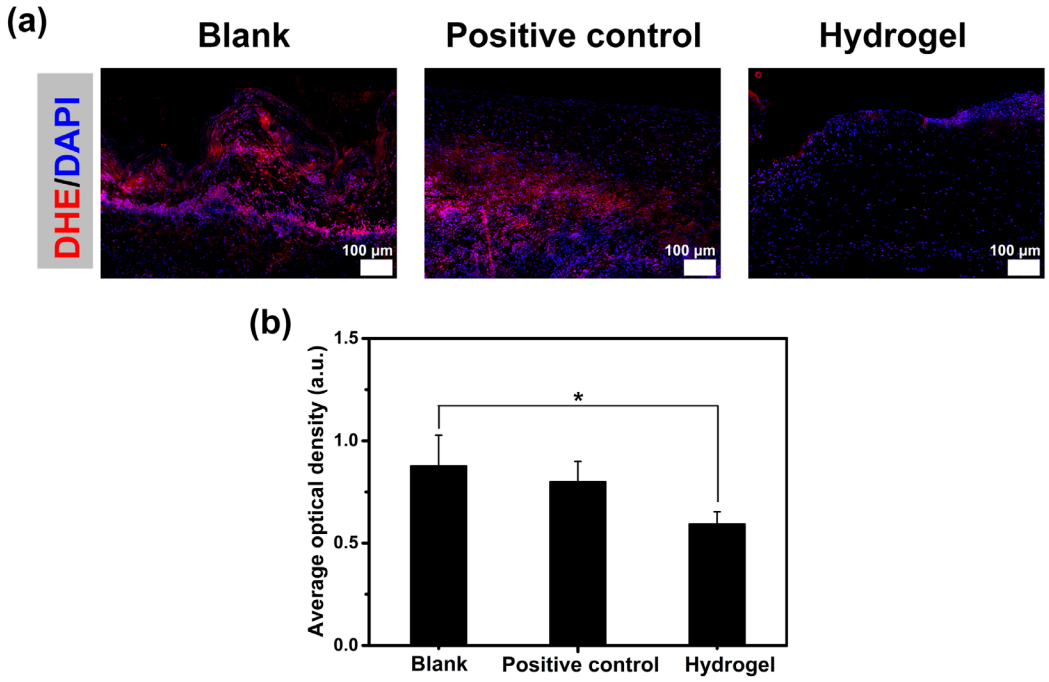

Fig. S10. (a) DHE staining to measure ROS at the wound sites after different treatments for 2 d (DHE: red color; DAPI: blue color). (b) Average optical density of DHE fluorescence corresponding to the different treatment in (a).

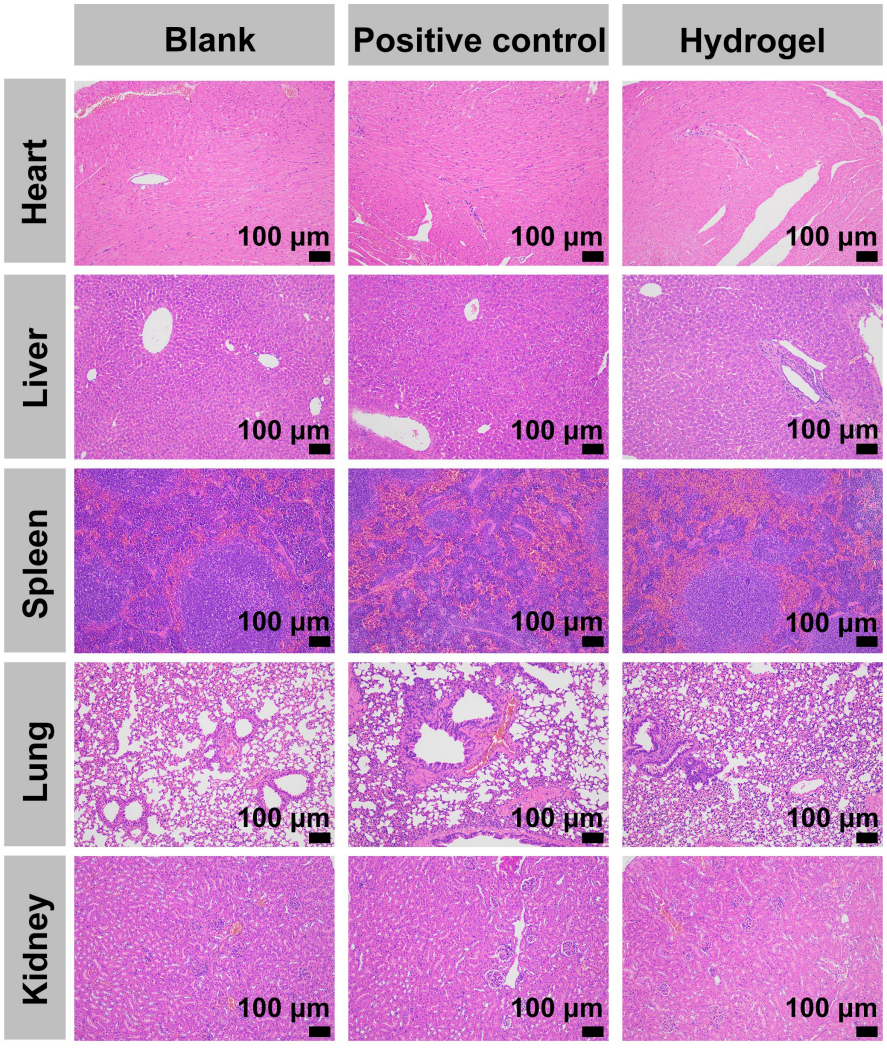

Fig. S11. H&E staining images of the major organs from mice after different treatments (12 days after treatment).

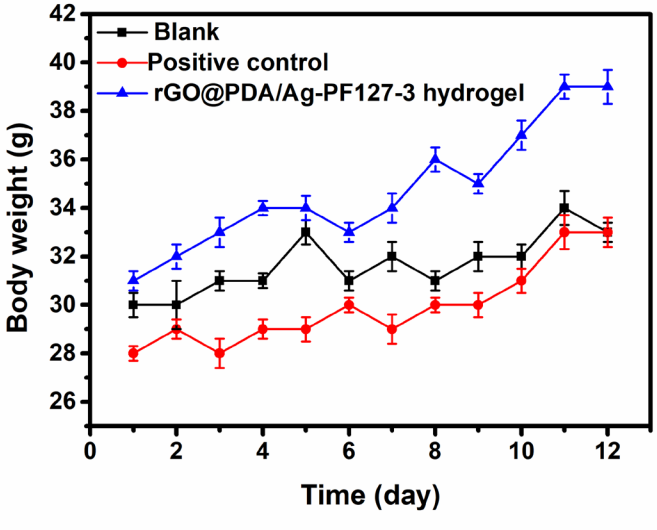

Fig. S12. The body weight changes of mice with different treatments during 12 days. Data are shown as mean ± SD, n = 3.

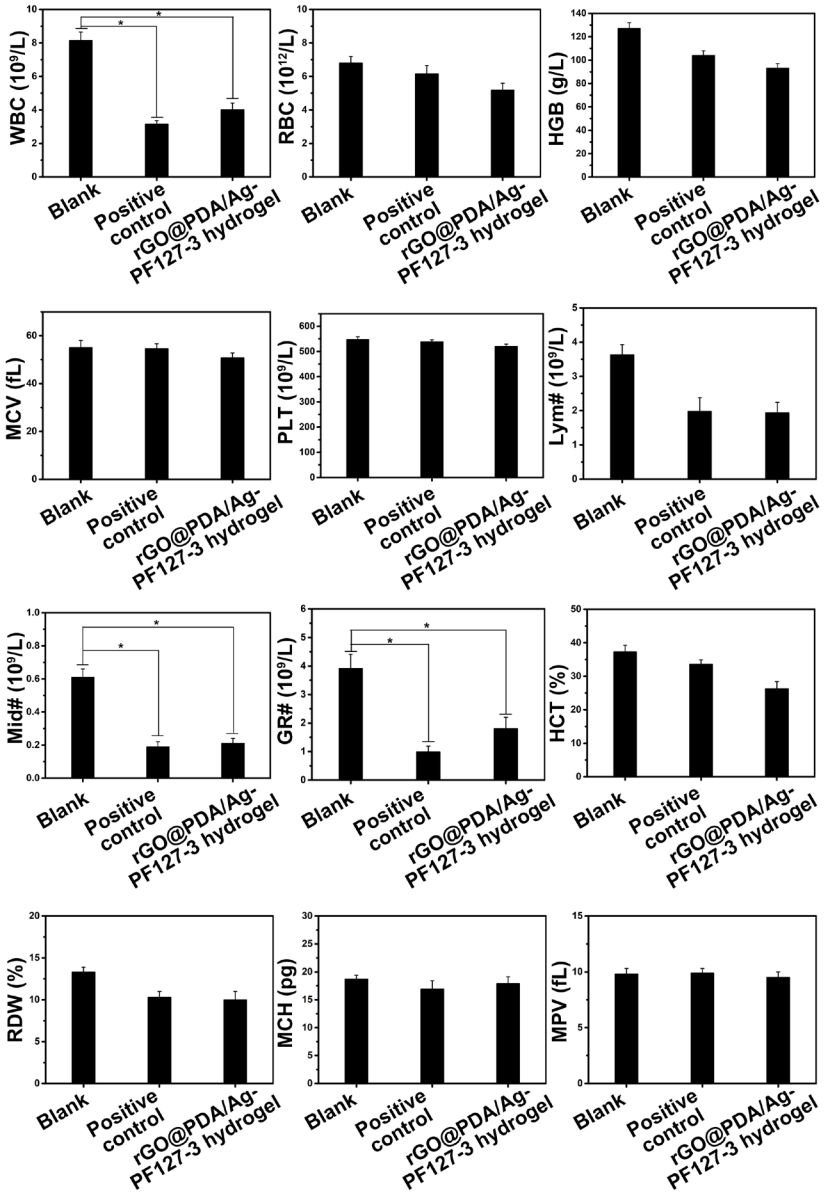

Fig. S13. Data of standard hematology from different groups on day 12, including white blood cell (WBC), red blood cell (RBC), hemoglobin (HGB), mean corpuscular volume (MCV), platelet (PLT), lymphocytes (Lymp#), monocytes (Mid#), granulocytes (Gr#), hematocrit (HCT), red cell distribution width (RDW), mean corpuscular hemoglobin (MCH), and mean platelet volume (MPV). Data are shown as mean ± SD, n = 3.

Video caption: Video S1 Hydrogel removal from a wound bed by cooling-induced gel-sol phase change.